

The architecture of Rhodobacter sphaeroides chromatophores

Simon Scheuring, Reinat Nevo, Lu-Ning Liu, Stéphanie Mangenot, Dana Charuvi, Thomas Boudier, Valerie Prima, Pierre Hubert, James N. Sturgis, Ziv Reich

▶ **To cite this version:**

Simon Scheuring, Reinat Nevo, Lu-Ning Liu, Stéphanie Mangenot, Dana Charuvi, et al.. The architecture of Rhodobacter sphaeroides chromatophores. Biochimica biophysica acta (BBA) - Bioenergetics, 2014, 1837, pp.1263-1270. 10.1016/j.bbabio.2014.03.011 . inserm-01356860

HAL Id: inserm-01356860

https://inserm.hal.science/inserm-01356860

Submitted on 26 Aug 2016

HAL is a multi-disciplinary open access archive for the deposit and dissemination of scientific research documents, whether they are published or not. The documents may come from teaching and research institutions in France or abroad, or from public or private research centers.

L'archive ouverte pluridisciplinaire **HAL**, est destinée au dépôt et à la diffusion de documents scientifiques de niveau recherche, publiés ou non, émanant des établissements d'enseignement et de recherche français ou étrangers, des laboratoires publics ou privés.

Biochimica et Biophysica Acta 1837 (2014) 1263–1270

Contents lists available at ScienceDirect

Biochimica et Biophysica Acta

journal homepage: www.elsevier.com/locate/bbabio

The architecture of *Rhodobacter sphaeroides* chromatophores

Simon Scheuring [a,*], Reinat Nevo [b], Lu-Ning Liu [a,1], Stéphanie Mangenot [c], Dana Charuvi [b], Thomas Boudier [d], Valerie Prima [e], Pierre Hubert [e], James N. Sturgis [e], Ziv Reich [b]

[a] U1006 INSERM, Aix-Marseille Université, Parc Scientifique de Luminy, Marseille F-13009, France
[b] Department of Biological Chemistry, Weizmann Institute of Science, Rehovot 76100, Israel
[c] UMR168 CNRS, Institut Curie, 26 rue d'Ulm, 75005 Paris, France
[d] Sorbonne Universités, UPMC Univ Paris 06, IBPS, F-75005 Paris, France
[e] LISM CNRS, Aix-Marseille Université, 31 Chemin Joseph Aiguier, 13402 Marseille, France

ARTICLE INFO

Article history:
Received 9 February 2014
Received in revised form 17 March 2014
Accepted 24 March 2014
Available online 28 March 2014

Keywords:
Electron tomography
Atomic force microscopy
Membrane structure
Reaction center
Light-harvesting complex

ABSTRACT

The chromatophores of *Rhodobacter* (*Rb.*) *sphaeroides* represent a minimal bio-energetic system, which efficiently converts light energy into usable chemical energy. Despite extensive studies, several issues pertaining to the morphology and molecular architecture of this elemental energy conversion system remain controversial or unknown. To tackle these issues, we combined electron microscope tomography, immuno-electron microscopy and atomic force microscopy. We found that the intracellular *Rb. sphaeroides* chromatophores form a continuous reticulum rather than existing as discrete vesicles. We also found that the cytochrome bc_1 complex localizes to fragile chromatophore regions, which most likely constitute the tubular structures that interconnect the vesicles in the reticulum. In contrast, the peripheral light-harvesting complex 2 (LH2) is preferentially hexagonally packed within the convex vesicular regions of the membrane network. Based on these observations, we propose that the bc_1 complexes are in the inter-vesicular regions and surrounded by reaction center (RC) core complexes, which in turn are bounded by arrays of peripheral antenna complexes. This arrangement affords rapid cycling of electrons between the core and bc_1 complexes while maintaining efficient excitation energy transfer from LH2 domains to the RCs.

© 2014 Elsevier B.V. All rights reserved.

1. Introduction

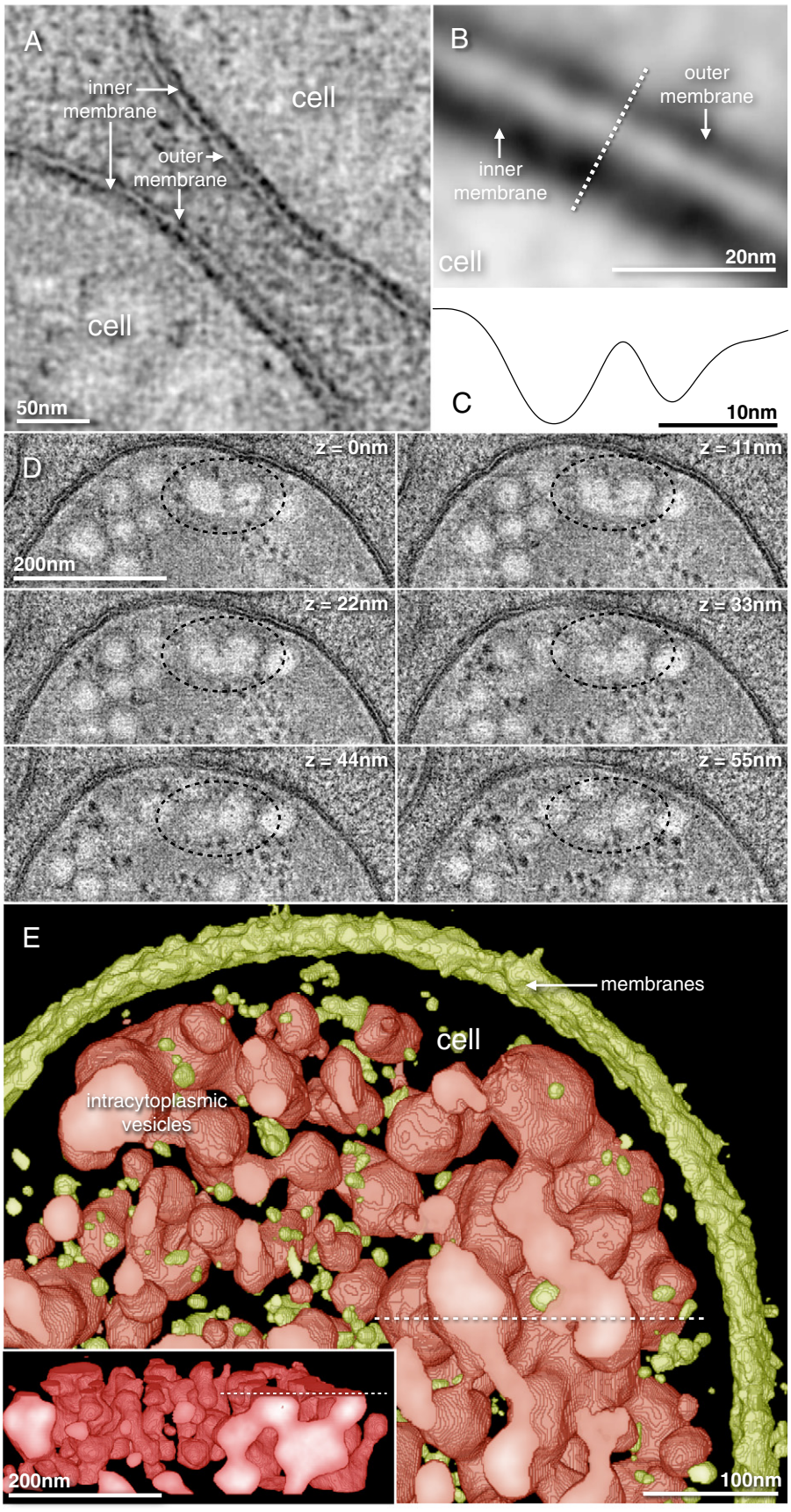
All of the components required for anaerobic photosynthesis in the purple bacteria *Rhodobacter* (*Rb.*) *sphaeroides* are found within specialized intracytoplasmic vesicles termed chromatophores. The peripheral light-harvesting complex 2 (LH2), typically arranged in nonameric rings, captures photons via non-covalently linked pigments [1]. The absorbed light energy is then converted into excitation energy and is transferred from one complex to another on a time scale of picoseconds [2]. Eventually, it arrives at light-harvesting complex 1 (LH1), which surrounds the reaction center (RC) [3]. Together, LH1 and the RC form the so-called core complex [4,5], where charge separation takes place. Following two photochemical cycles, a quinone is fully reduced to quinol and diffuses in the membrane plane until it reaches the cytochrome bc_1 complex [6]. The dimeric bc_1 complex re-oxidizes the quinol, through a Q-cycle mechanism [7], and the electrons are shuttled back via soluble cytochrome c_2 to the RC. Concomitantly, the bc_1 complex liberates protons into the internal chromatophore lumen, which are utilized by ATP synthase to generate ATP [8].

While the composition of *Rb. sphaeroides* photosynthetic apparatus and the structure of its individual pigment–protein complexes are well characterized, some key issues pertaining to its macroscopic organization and the details of its operation remain unclear. Nowadays, the view that the chromatophores in *Rb. sphaeroides* exist as discrete vesicles is often accepted. However, historically, connectivity between the vesicular chromatophores has been proposed as early as 1965 based on electron microscopy and biochemical analysis [9–11]. The organization of the chromatophore membranes either as discrete vesicles or as a connected reticulum or network should have important implications for its function, maintenance as well as for its biogenesis. The supramolecular organization of the complexes that mediate light harvesting and electron transport is likewise under debate, and so is the contribution of the different complexes to the membrane curvature required to initiate budding of the chromatophores from the cell membrane from which they originate [12–14]. Atomic force microscopy (AFM) has been performed on chromatophores of various species, and proved invaluable for elucidating the organization of the light-harvesting apparatus (for a review, see [15]). Polarized spectroscopy and modeling have likewise made important contributions to our understanding of the supramolecular organization of the *Rb. sphaeroides* chromatophore system and its

* Corresponding author.
E-mail address: simon.scheuring@inserm.fr (S. Scheuring).
[1] Present address: Institute of Integrative Biology, Bioscience Building, University of Liverpool, Crown Street, Liverpool L69 7ZB, UK.

http://dx.doi.org/10.1016/j.bbabio.2014.03.011
0005-2728/© 2014 Elsevier B.V. All rights reserved.

biogenesis [16,17]. However, there are still unanswered questions concerning the supramolecular organization of the complexes, particularly in the case of *Rb. sphaeroides*, where the vesicular structures need to be flattened for AFM analysis [18–20]. Finally, until very recently, the localization of the bc_1 complex within the chromatophore membranes has been unknown, in all anaerobic



phototrophs [20,21], including *Rb. sphaeroides* [18]. While submitting this manuscript, we became aware of another study [22], in which the bc_1 complex was localized in isolated *Rb. sphaeroides* chromatophores.

In order to address the above issues, we combined electron microscope tomography (EMT), immuno-electron microscopy (immuno-EM), as well as AFM analysis of native chromatophore membranes. The results obtained from the studies shed new light on the organization of the chromatophore membranes of *Rb. sphaeroides* and on the organization of the protein complexes within them, providing important insight into their function.

2. Results

To study the morphology of *Rb. sphaeroides* chromatophores in three dimensions in situ, we performed dual-axis EMT analysis on sections obtained from high-pressure frozen, freeze-substituted samples, as described [23–26]. As can be seen (Fig. 1A), the inner and outer cell membranes are well resolved in the tomograms. The two membranes (Fig. 1B) are separated from each other by about 5 nm and have an apparent thickness of ~7 and ~5 nm, respectively (Fig. 1C). The inner membrane appears significantly denser than the outer, likely due to the high density of peripheral proteins in the former. The chromatophores seen in the tomographic slices (Fig. 1D) appear as separate spherical objects averaging 50 ± 20 nm in diameter. This conforms to the view that the chromatophores in *Rb. sphaeroides* exist primarily as discrete, autonomous bodies. However, following segmentation and rendering of the reconstructed volume, it becomes clear that the chromatophores are, in fact, fused to each other at different, often multiple, points, with the connecting regions varying in diameter (Fig. 1E). The result is a continuous, three-dimensional (3D) vesiculated network or reticulum that persists throughout the entire cytoplasmic space and occupies a significant fraction of its volume. In contrast to the results obtained in a recent cryo-EMT study [14], we did not detect connections between the inner cell membrane and the chromatophore membranes. In their report, Tucker et al. proposed that the number of connections between the chromatophores and the cell membrane may depend on growth light intensity and developmental state. The absence of such connections in our samples may be due to the fact that the cells examined by us had fully matured chromatophore membranes, whereas the chromatophores in the cells examined by Tucker et al. appear to be in an earlier developmental stage (see Fig. 6 in Ref. [14]). It is also possible, however, that we did not detect chromatophore–cell membrane connections because these were poorly contrasted by heavy metal staining of the freeze-substituted samples.

We also addressed the issue of where the cytochrome bc_1 complex is localized in the chromatophore membranes. As mentioned in the Introduction, the localization of this complex, along with that of the ATP synthase, within the photosynthetic membranes of anoxygenic phototrophs remains enigmatic (for a review see [20]; but see Cartron et al. [22] in this issue). Recently, we were able to demonstrate possible long-range quinone pathways in the lamellar chromatophores of *Rhodospirillum* (*Rsp.*) *photometricum* [21]. Within this framework, the bc_1 complex was postulated to localize at the edges of the lamellae and at invagination sites of the chromatophore membranes [21]. Following similar considerations, the bc_1 complex of *Blastochloris* (*Blc.*) *viridis* was likewise proposed to be located at the highly curved edges of the lamellar stacks that constitute the chromatophore unit of this organism [27]. To obtain information on the localization of the bc_1 complex in *Rb. sphaeroides* chromatophores, we performed immuno-EM analysis of isolated chromatophores; attempts to label the complex on sections obtained from cell suspensions unfortunately failed. The isolation and EM preparation procedures resulted in breakage of the connections between the chromatophores, yielding separate vesicles (Fig. 2A). Four labeling patterns were observed: (i) the gold particle was on top of the chromatophore vesicle (termed 'vesicle', 1st column in Fig. 2A), (ii) the label was on a membrane structure that protrudes out of the vesicle ('neck', 2nd column in Fig. 2A), (iii) the label was on a small membrane fragment ('fragment', 3rd column in Fig. 2A) and (iv) two closely associated gold particles ('aggregates', 4th column in Fig. 2A). The relative abundance of these labeling characteristics (n = 260) was: 'vesicle': 15.0% ± 2.4%; 'neck': 35.8% ± 3.7%; 'fragment': 39.2% ± 3.9%; and 'aggregates': 5.0% ± 1.4% (Fig. 2B). This distribution suggests that the bc_1 complex resides primarily in fragile membrane regions, accounting for the fact that a total of ~45% ('fragment' + 'aggregates') of the labels were present on small, dissociated membrane fragments and that an additional 36% of the labels were present on membrane regions that protruded out of the vesicles ('necks'). Assuming that the 'fragment' and 'aggregate' fractions were neck regions that had detached from the main chromatophore body during isolation or preparation for EM, about 80% of the labels thus represent neck regions. We further propose that at least some of the labels seen on the main vesicle body (Fig. 2A, 1st column) correspond to neck regions that had collapsed onto the vesicle surface.

In order to obtain information on the molecular constituents and organization of chromatophore membranes, we performed AFM analysis on isolated vesicles. To maximally preserve their native state, the analysis was performed on samples that were not pre-treated with detergent. Imaging the vesiculated chromatophores (Fig. 3A) was very challenging and required particular attention to the force applied to the sample [28–32]. Despite these efforts, imaging of large membrane areas was not possible and the resolution was partially compromised, when compared to samples from species with lamellar intracytoplasmic membranes such as *Rhodopseudomonas* (*Rps.*) *viridis* [33], *Rsp. photometricum* [21,34–38], and *Rhodopseudomonas palustris* [39]. Rather, we were only able to visualize small membrane patches at peripheral regions of the vesicles close to the support surface, probably because of the greater membrane stiffness of these regions compared to the dome regions. Although the resolution we obtained was lower than that obtained for intracytoplasmic membranes of other species [20], we were nonetheless able to reproducibly detect molecular clusters consisting of about ten protein complexes. A frequently observed assembly pattern at the highly curved peripheral membrane regions was that of hexagonally packed LH2 complexes (Fig. 3B), similar to what we had observed in *Rsp. photometricum* [34] and *Phaeospirillum molischianum* [31]. This arrangement has been suggested by molecular dynamics simulations (MDS) to induce membrane curvature in vesiculated chromatophores [40]. It is also known that, in *Rb. sphaeroides*, LH2 complexes are sufficient to induce membrane curvature and indeed can assemble chromatophores in core-deficient mutants [41]. Rarely, we detected LH2 assemblies significantly larger than the typically observed nonameric form, possessing a ring diameter of about 100 Å (Fig. 3B, arrow), as found in *Rsp. photometricum* [34] and *Phsp. molischianum* [31]. No indication for the presence of LH2 dimers [18,32,42] or RC–LH1–PufX dimer rows [18] was obtained from the membrane regions observed in this study.

Fig. 1. Architecture of the cell and chromatophore membranes of *Rb. sphaeroides*. A) Tomographic slice (5.5-nm thick) depicting the membranes of two *Rb. sphaeroides* cells. The inner and outer membranes are clearly discernable. B) The cell membranes as seen in a thicker (33 nm) slice perpendicular to the membrane plane of the reconstructed volume. The inner membrane, the permeability barrier, appears much more contrasted than the porin-dense outer membrane. C) Gray-scale profile taken across the cell membranes along the dashed line in (B). The measured thicknesses of the inner and outer membranes are ~7 nm and ~5 nm, respectively. D) A series of slices at different z-positions of the tomographic volume illustrating the vesicular appearance of intracytoplasmic membranes in *Rb. sphaeroides* when visualized in 2D. Nonetheless, interconnections between neighboring chromatophore bodies are observed (dashed outlines). E) Model, generated from the tomographic data, showing the cell and chromatophore membranes (colored in light green and brown-red, respectively). Inset: A slice through the 3D model along the dashed line shown in the main panel, showing only the chromatophore membranes. As can be seen, the chromatophores are fused to each other at multiple points, forming a continuous tubular network or reticulum within the cell.

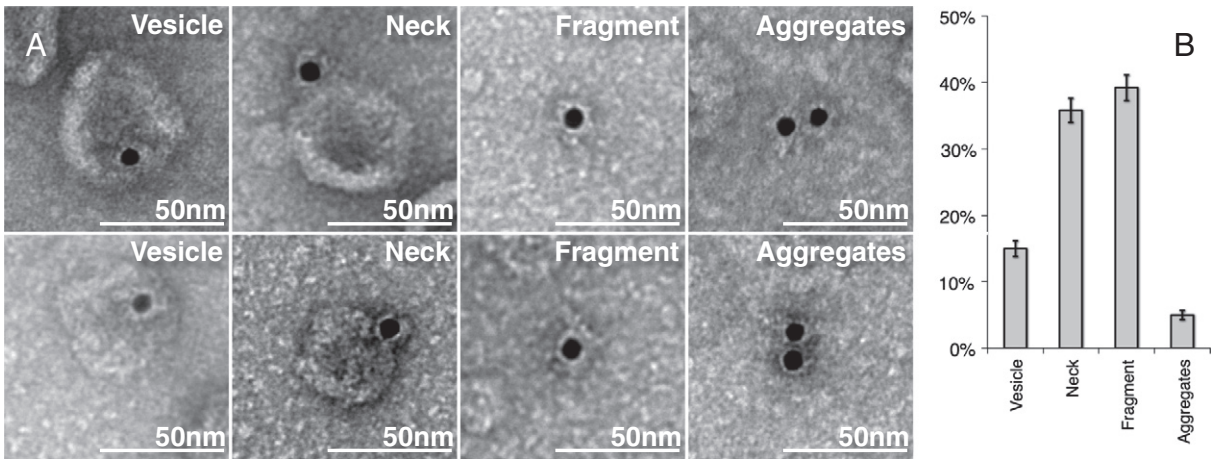


Fig. 2. Labeling of the cytochrome bc_1 complex on isolated *Rb. sphaeroides* chromatophores. A) Electron micrographs displaying labels on chromatophore "vesicles", on "neck" regions that protrude out of the vesicles, and on small membrane "fragments". The right-most column shows membrane fragments that were doubly labeled, which we refer to as "aggregates". B) Abundance of the four classes of labeling. The majority of labels are found on vesicle "necks" and on detached small "fragments".

3. Discussion

In this study we combined several imaging techniques to characterize the morphology and ultrastructure of the chromatophore membranes of *Rb. sphaeroides*. The results we obtained from the EMT studies indicate that the chromatophore vesicles of *Rb. sphaeroides* are fused to each other at multiple points by membrane constrictions, forming a continuous reticulum that encloses a single luminal space, similar to the organization of oxygenic photosynthetic (thylakoid) membranes [23–25,43]. Such connectivity is advantageous as it allows the system to respond to internal or external cues in a concerted manner. It also simplifies the trafficking of material into or out of the system, as only a few entry or

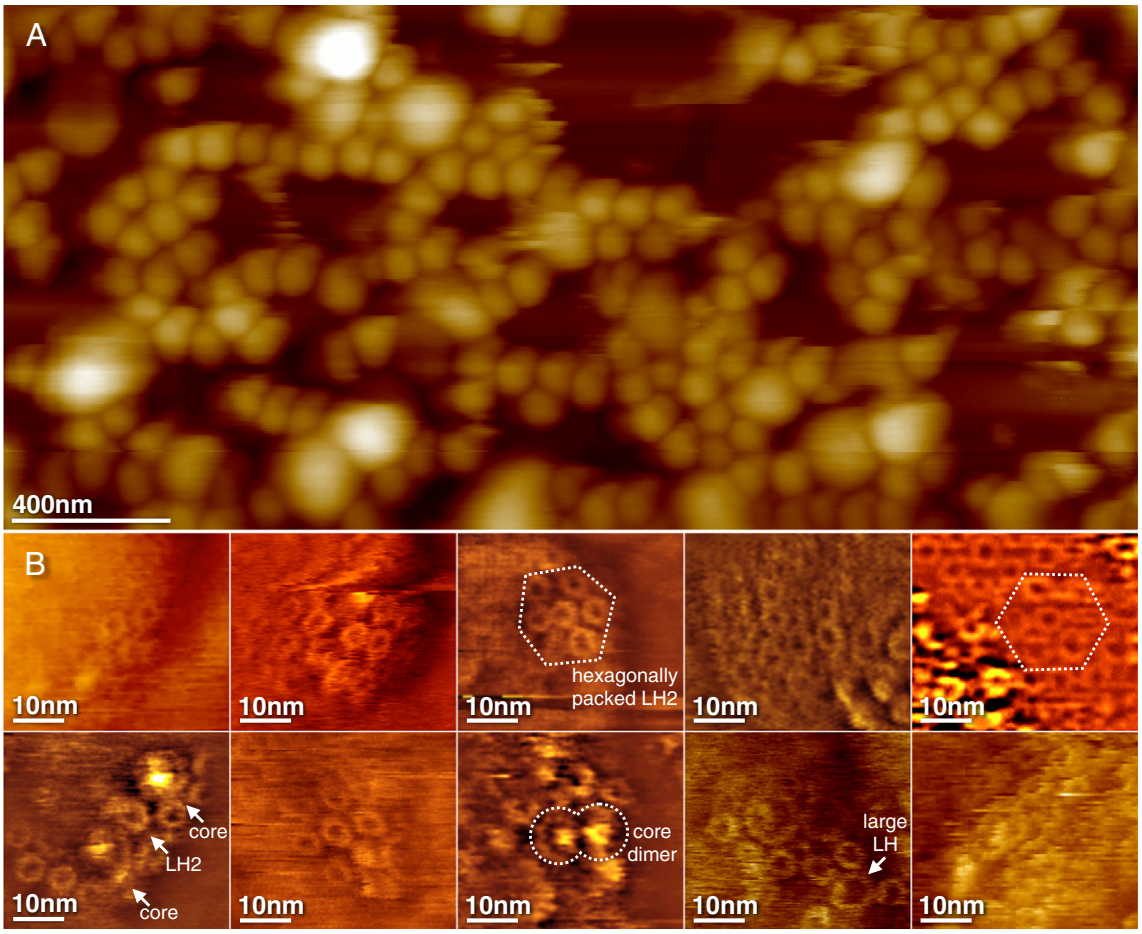


Fig. 3. Organization of protein complexes in the intracytoplasmic membranes of *Rb. sphaeroides* visualized in isolated chromatophores. A) Low-magnification AFM topograph of purified vesicular chromatophores adsorbed to a mica support. As no detergent was added, the chromatophores preserved their native spherical shape and did not flatten on the supporting substrate. B) Molecular-resolution topographs showing assemblies of core and LH2 complexes. The latter often exhibit hexagonal arrangement (dashed outlines). Occasionally larger LH2 complexes can be seen (arrow).

exit points are required, therefore simplifying its formation and maintenance. The fact that, rather than existing as isolated spherical bodies, the chromatophores of *Rb. sphaeroides* are organized in complex reticular networks may also have important implications for studies aiming at modeling light harvesting and electron transport in the chromatophore system, as well as the conversion of the captured light energy to chemical energy through the dissipation of transmembrane proton motive force generated during the transport reactions (e.g., [17,44]).

Despite early reports suggesting an interconnected chromatophore system in purple bacteria [11,45], in recent years the concept of discrete chromatophore vesicles has prevailed [44]. This view gained substantial support from 2D projection images obtained from thin-section electron micrographs of cells or isolated chromatophores [9,10,12–14,46]. As the number of connections present between neighboring vesicles is small and as they are apparently randomly oriented, in projection, the chromatophores would appear mostly as separate, circularly delineated objects. Indeed, when single tomographic slices are examined, the chromatophores appear mostly as isolated vesicles (Fig. 1D); their interconnected nature is best revealed when volume rendering and segmentation of the tomographic volume is carried out. In addition, the connections that link the chromatophores to each other likely break during isolation, as we observed when we prepared the samples for the immuno-EM and AFM studies. This is probably the case also for the connections between the chromatophores and the cytoplasmic membrane, as these are likely to be very labile as well ([14] and references therein).

Recently, Tucker and co-workers employed cryo-electron tomography to study chromatophore development in *Rb. sphaeroides* [14]. While tomograms were acquired on both thin/semi-thick sections and whole cells, segmentation and volume rendering of the chromatophores were performed only on tomograms recorded from the whole-cell samples, in which high-resolution information could be extracted only for regions adjacent to the cell membrane. In the latter case, the authors did observe some fused chromatophore clusters, but these clusters were proposed to represent secondary budding events that take place during biogenesis and that eventually break apart upon maturation. Inspecting a tomogram acquired by the authors from a semi-thick vitreous section (Supplemental movie S1 in [14]), where the chromatophores are well resolved throughout the cell volume, it appears that they are connected to each other in the central regions of the cell (where they should assume their final, mature form), similar to what we observed. It is thus likely that connectivity between chromatophores is a general feature of *Rb. sphaeroides*. As proposed by Tucker et al. for the connections between the chromatophores and the cell membrane, we propose that the extent of connectivity of the chromatophore network may also vary with light and/or other growth conditions.

Electron transport in the chromatophores requires the presence of cytochrome bc_1. While it has been suggested that the bc_1 complex is closely associated with the RC [47], its exact localization in the chromatophore membranes of *Rb. sphaeroides* or in the photosynthetic membranes of other anoxygenic phototrophs has remained elusive until now (see below). Here we were able to label cytochrome bc_1 complexes in isolated chromatophore membranes. Although the preparation of the chromatophore vesicles resulted in breakage of the connections between the chromatophore vesicles, complicating the analysis, the labeling patterns observed strongly suggest that the complexes localize to the fragile membrane regions that interconnect the chromatophores in the network. We have recently proposed that bc_1 resides at the peripheral edges of the chromatophore membranes of *Rsp. photometricum* [21]. Likewise, structural and spectroscopic analyses of the intracytoplasmic photosynthetic membranes of *Blc. viridis* led Konorty et al. [27] to suggest that bc_1 complexes are localized to the edges of the stacked lamellar sheets into which these membranes are organized. Most recently, EM and AFM combined with bc_1 gold labeling, has been performed to analyze the bc_1 localization within *Rb. sphaeroides* chromatophores [22]. It was concluded that the bc_1 complex mostly exists as dimers and resides adjacent to RC–LH1–PufX complexes.

AFM analysis of purified chromatophores revealed the typical vesicular morphology of isolated chromatophores, as documented previously by EM [9]. Earlier, the chromatophores of *Rb. sphaeroides* had been studied by AFM using a sample preparation technique that takes advantage of sub-solubilizing amounts of detergent to open and flatten the vesicles on the AFM mica support [18]. Here, we avoided any strategy for vesicle opening or flattening [19], limiting imaging resolution and the possibility to visualize large areas. Despite these limitations, we could acquire some molecular details on the spherical chromatophores, notably the hexagonal arrangement of LH2 complexes. Based on our data, we cannot confirm clustering of dimeric core complexes in arrays, as previously reported [17,18,44]. We only visualized few core complexes, some dimeric, as expected [48–50], and some apparently monomeric.

Finally, we propose a model for the organization of the photosynthetic protein complexes within the chromatophore network of *Rb. sphaeroides*. In constructing the model, we took into account the local curvature of the membranes, as derived from surface curvature analysis of the reconstructed chromatophore reticulum (Fig. 4), the localization of cytochrome bc_1 suggested by the immuno-EM data, the apparent preference of the reaction center and LH2 complexes for convex membrane domains [40,41,51–53], and the assumption that, for optimal efficiency, the reaction centers should lie in close proximity to both LH2 and cytochrome bc_1 complexes. In light of these, we propose that the cytochrome bc_1 complexes reside primarily in the concave and relatively flat 'neck' regions that interconnect the chromatophores in the network (Fig. 4, blue and white regions). These foci are surrounded by the RC–LH1–PufX core complexes (white regions and adjacent red regions), ensuring that diffusion distances of quinones/quinols and cytochrome c_2 proteins, which mediate electron transport between the reaction centers and the cytochrome bc_1 complexes, are minimized. The rest of the reticulum (red), which consists of high-curvature convex membrane domains, is occupied by LH2 complexes, consistent with these complexes being the most abundant components of the apparatus and their proposed role in membrane bending by molecular dynamics simulations [52]. This concentric arrangement should enable efficient cycling of electrons between the reaction centers and cytochrome bc_1 complexes without disturbing the transfer of excitation energy from the peripheral antennae to the reaction centers. The short distances between bc_1 complexes and RCs as predicted by the model (ca. 10 nm) are consistent with a previous work in which electron transport rates were estimated in *Rhodobacter capsulatus* containing different bc_1 fusions [54]. It is therefore expected to allow for efficient funneling of excitation energy to discrete, small loci that contain RC–LH1–PufX, quinones/quinols, cytochrome c_2, and cytochrome bc_1, minimizing the space for the diffusive electron transfer reactions that limit the overall rate of the process and, therefore, maximizing its speed and efficiency.

Our molecular model is essentially in agreement with the recent analysis of Cartron and colleagues [22], connecting the core complexes on one side to LH2 and on the other side to cytochrome bc_1 complexes, hence spatially separating excitation from electron transfer. It was observed by Cartron et al. [22], that the labels of the bc_1 complexes appeared mostly in clusters. This, too, is consistent with our model in which the bc_1 complexes localize to the regions that interconnect the vesicles in the reticulum. Since these fragile regions break during chromatophore isolation, the appearance of clustered bc_1 labeling would be expected. This is especially evident in the labeling of flattened isolated chromatophore vesicles in their work. As Cartron et al. utilized a 10-His–bc_1 fusion strain for their labeling, they had the advantage of being able to achieve multiple labeling, including dimeric complexes. We note that our labeling pattern, which was carried out with an antibody against a part of native bc_1 and thus may have not been able to double-label dimeric complexes due to steric problems, does not exclude the possibility that the complexes exist as dimers in the

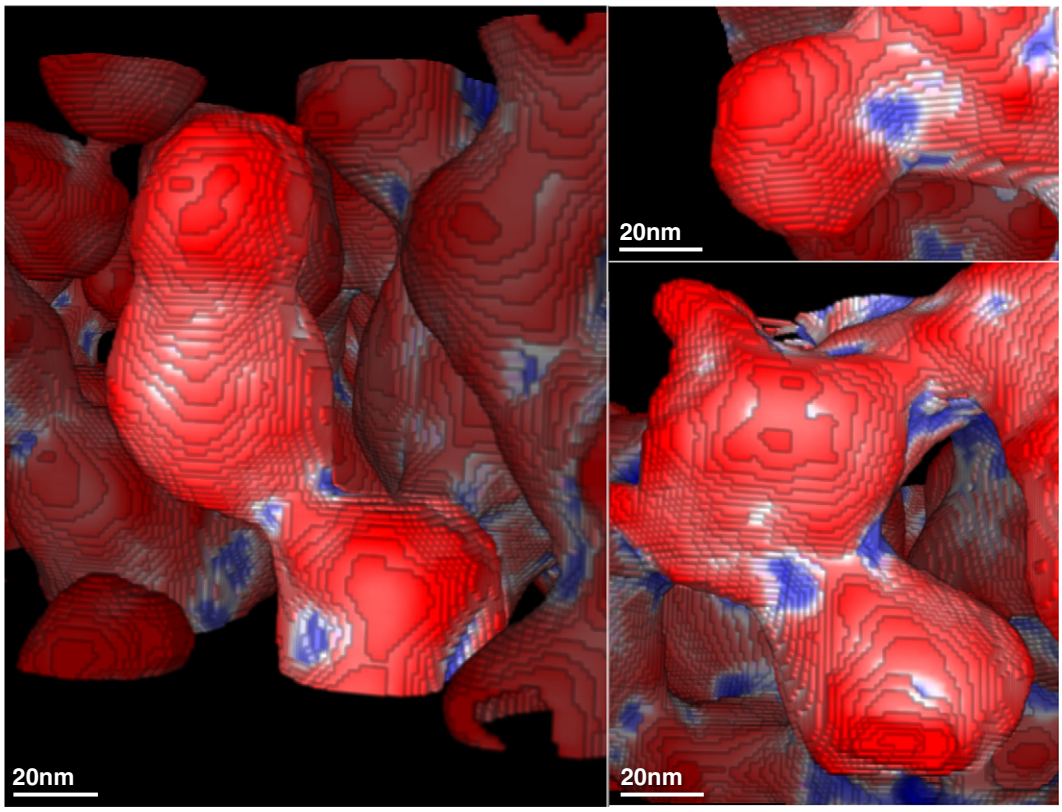


Fig. 4. The chromatophore network of *Rb. sphaeroides* color-rendered according to its local (10-nm) curvature. Concave and convex regions are colored in blue and red, respectively, and the relatively flat regions in between are shown in white. We propose that the cytochrome bc_1 complexes reside in the concave and flat membrane surfaces that are found mostly at the regions that interconnect the chromatophores. These complexes are surrounded by RC–LH1–PufX core complexes, which in turn are surrounded by the peripheral LH2 antennae, both of which localize to the convex regions that constitute most of the reticulum surface. This arrangement permits efficient funneling of excitation energy to the RC–LH1–PufX-rich loci while maintaining the latter in close proximity to the bc_1 complexes, thus facilitating the shuttling of electrons between the two.

membranes. However, our models differ with regard to the overall chromatophore organization *in vivo*, vesicles versus a reticulated system. Both models fail to account for functional measurements suggesting slow electron transfer rate in LH2 enriched membranes [55], as the LH2s should be confined to membrane regions that are not perfused by electron carriers.

4. Materials and methods

4.1. Growth and harvesting

Rb. sphaeroides Ga strain cells were grown anaerobically in modified Hutner medium [56] with illumination from a tungsten lamp at a moderate light-intensity of ~30 W/m^2, and harvested in late log phase. Prior to preparation for the EM examinations, the cells were washed two times with cold 10 mM Tris–HCl pH 8.0.

4.2. Transmission electron microscopy and tomography

Sample preparation, imaging, and data processing were as described in [24]. Dual-axis electron tomography was performed on semi-thick sections obtained from high-pressure frozen, freeze-substituted samples, as described in [23–26]. For a recent comparison of images obtained by this method to those recorded by cryo-EM on vitreous sections, see Kirchhoff et al. [57]. Segmentation and surface rendering of the cells and chromatophore membranes were performed using JAVA routines [58] for the Image-J image processing platform [59].

4.3. Chromatophore purification and purified chromatophore analysis

Chromatophores were isolated as described previously [60] from *Rb. sphaeroides* Ga strain grown to late log phase. Cells were collected and washed in 1 mM Tris–HCl (pH 7.5), and resuspended in the same buffer. DNAase (0.1 mg/ml final concentration) was added to the cell slurry that was subsequently passed (once) through a French pressure cell operating at 1000 psi. The lysate (collected on ice) was centrifuged briefly (15 min at 2500 g) to remove unbroken cells prior to layering on a continuous 5–35% sucrose density gradient poured over a 60% sucrose cushion and centrifuged for 90 min at 27,000 rpm in a SW28 rotor. Chromatophores were isolated from a strongly colored band at about 25% sucrose. The sucrose was then removed from the chromatophore suspension by two-fold dilution with 1 mM Tris–HCl (pH 7.5) and pelleting by ultra-centrifugation.

4.4. Atomic force microscopy

Nanoscope-E and Nanoscope-V AFMs [61] (Bruker, Santa Barbara, CA, USA), equipped with a 160-μm scanner (J-scanner) and oxide-sharpened Si_3N_4 cantilevers (length 100 μm; $k = 0.09$ N/m; Olympus Ltd., Tokyo, Japan) were operated in contact mode at ambient temperature and pressure. For imaging, minimal loading forces of ~100 pN were applied, at scan frequencies of 4–7 Hz, using optimized feedback parameters. The mica supports were immersed in 40 μl of adsorption buffer (10 mM Tris–HCl, 150 mM KCl, 25 mM $MgCl_2$, pH 7.5). Subsequently, 2 μl of a solution containing isolated chromatophore membranes was injected into the buffer drop. After one hour or so the sample was rinsed

with recording buffer (10 mM Tris–HCl, 150 mM KCl, pH 7.5) before imaging.

4.5. Immuno-electron microscopy

Antibodies against the cytochrome bc_1 complex were provided by Eurogentec (Seraing, Belgium). These antibodies were raised against two peptides (CYYGSYKPPREVLW and CSNNPLGIDAKGPFDT), corresponding to regions present within the putative cytoplasmic loops of the cytochrome *b* subunit of *Rhodospirillum rubrum*. Several parts of these sequences are well conserved in the cytochrome *b* of *Rb. sphaeroides*, and the antibodies detect the cytochrome *b* of *Rb. sphaeroides* in Western blots (not shown). All steps of the immuno-labeling were carried out at room temperature in a closed and humidified environment by floating grids on drops of the different solutions. Purified chromatophore samples of *Rb. sphaeroides* (5 μl) were adsorbed onto carbon-coated, glow discharged copper grids (300 mesh, EMS, Hatfield, USA) for 5 min. The adsorbed *Rb. sphaeroides* chromatophores were washed twice with PBS containing 1% BSA, to remove unadsorbed membranes. The grids were then incubated for 30 min with anti-cytochrome bc_1 diluted 1/100, 1/200 and 1/300 times in PBS containing 1% BSA buffer. Negative control was performed by incubation with pre-immune serum for 30 min. All grids were then washed (5×) with PBS containing 0.1% BSA and were then incubated with gold-labeled protein A (10 nm; CMC, Utrecht, Netherlands; 1/75) for 20 min. The grids were then washed with PBS/0.1% BSA, then with only PBS and, finally, with water. Samples were stained for 30 s with 2% uranyl acetate and were visualized with a Philips CM12 operating at 120 kV.

Acknowledgements

Work in the Scheuring lab was supported by a European Research Council (ERC) Starting Grant (# 310080), and an Agence National de la Recherche (ANR) grant (# ANR-12-BSV8-0006-01). Work in the Sturgis lab was supported by an Agence National de la Recherche (ANR) grant (# BLAN07-1_183779). Work in the Reich lab was supported by grants from the Israel Science Foundation (No. 1034/12) and the Minerva Foundation (Federal German Ministry for Education and Research, No. 710819). Thin-section electron microscopy and electron tomography studies were conducted at the Irving and Cherna Moskowitz Center for Nano and Bio-Nano Imaging at the Weizmann Institute of Science. Immuno-electron microscopy experiments were performed at the Imagopole platform at the Institut Pasteur, Paris, France.

References

[1] G. McDermott, S.M. Prince, A.A. Freer, A.M. Hawthornthwaite-Lawless, M.Z. Papiz, R.J. Cogdell, N.W. Isaacs, Crystal structure of an integral membrane light-harvesting complex from photosynthetic bacteria, Nature 374 (1995) 517–521.
[2] X. Hu, T. Ritz, A. Damjanovic, F. Autenrieth, K. Schulten, Photosynthetic apparatus of purple bacteria, Q. Rev. Biophys. 35 (2002) 1–62.
[3] J. Deisenhofer, O. Epp, K. Miki, R. Huber, H. Michel, Structure of the protein subunits in the photosynthetic reaction centre of *Rhodopseudomonas viridis* at 3 Å resolution, Nature 318 (1985) 618–624.
[4] A.W. Roszak, T.D. Howard, J. Southall, A.T. Gardiner, C.J. Law, N.W. Isaacs, R.J. Cogdell, Crystal structure of the RC–LH1 core complex from *Rhodopseudomonas palustris*, Science 302 (2003) 1969–1972.
[5] S. Scheuring, AFM studies of the supramolecular assembly of bacterial photosynthetic core-complexes, Curr. Opin. Chem. Biol. 10 (2006) 387–393.
[6] E.A. Berry, L.S. Huang, L.K. Saechao, N.G. Pon, M. Valkova-Valchanova, F. Daldal, X-ray structure of *Rhodobacter capsulatus* cytochrome bc(1): comparison with its mitochondrial and chloroplast counterparts, Photosynth. Res. 81 (2004) 251–275.
[7] J.W. Cooley, D.W. Lee, F. Daldal, Across membrane communication between the Q(o) and Q(i) active sites of cytochrome bc(1), Biochemistry 48 (2009) 1888–1899.
[8] J.E. Walker, ATP synthesis by rotary catalysis (Nobel lecture), Angew. Chem. Int. Ed. 37 (1998) 2308–2319.
[9] K.D. Gibson, Isolation and characterization of chromatophores from *Rhodopseudomonas sphaeroides*, Biochemistry 4 (1965) 2042–2051.
[10] J. Oelze, G. Drews, Membranes of photosynthetic bacteria, Biochim. Biophys. Acta 265 (1972) 209–239.
[11] R.C. Prince, A. Baccarini-Melandri, G.A. Hauska, B.A. Melandri, A.R. Crofts, Asymmetry of an energy transducing membrane. The location of cytochrome c2 in *Rhodopseudomonas spheroides* and *Rhodopseudomonas capsulata*, Biochim. Biophys. Acta 387 (1975) 212–227.
[12] K.D. Gibson, B.J. Segen, R.A. Niederman, Membranes of *Rhodopseudomonas spheroides*: II. Precursor–product relations in anaerobically growing cells, Arch. Biochem. Biophys. 152 (1972) 561–568.
[13] R.A. Niederman, B.J. Segen, K.D. Gibson, Membranes of *Rhodopseudomonas spheroides*: I. Isolation and characterization of membrane fractions from extracts of aerobically and anaerobically grown cells, Arch. Biochem. Biophys. 152 (1972) 547–560.
[14] J.D. Tucker, C.A. Siebert, M. Escalante, P.G. Adams, J.D. Olsen, C. Otto, D.L. Stokes, C.N. Hunter, Membrane invagination in *Rhodobacter sphaeroides* is initiated at curved regions of the cytoplasmic membrane, then forms both budded and fully detached spherical vesicles, Mol. Microbiol. 76 (2010) 833–847.
[15] L.-N. Liu, S. Scheuring, Investigation of photosynthetic membrane structure using atomic force microscopy, Trends Plant Sci. 18 (2013) 277–286.
[16] R.N. Frese, J.C. Pàmies, J.D. Olsen, S. Bahatyrova, C.D. van der Weij-de Wit, T.J. Aartsma, C. Otto, C.N. Hunter, D. Frenkel, R. van Grondelle, Protein shape and crowding drive domain formation and curvature in biological membranes, Biophys. J. 94 (2008) 640–647.
[17] M.K. Şener, J.D. Olsen, C.N. Hunter, K. Schulten, Atomic-level structural and functional model of a bacterial photosynthetic membrane vesicle, Proc. Natl. Acad. Sci. U. S. A. 104 (2007) 15723–15728.
[18] S. Bahatyrova, R.N. Frese, C.A. Siebert, J.D. Olsen, K.O. van der Werf, R. van Grondelle, R.A. Niederman, P.A. Bullough, C. Otto, C.N. Hunter, The native architecture of a photosynthetic membrane, Nature 430 (2004) 1058–1062.
[19] S. Scheuring, J. Busselez, D. Levy, Structure of the dimeric PufX-containing core complex of *Rhodobacter blasticus* by in situ atomic force microscopy, J. Biol. Chem. 280 (2005) 1426–1431.
[20] S. Scheuring, J.N. Sturgis, Atomic force microscopy of the bacterial photosynthetic apparatus: plain pictures of an elaborate machinery, Photosynth. Res. 102 (2009) 197–211.
[21] L.N. Liu, K. Duquesne, J.N. Sturgis, S. Scheuring, Quinone pathways in entire photosynthetic chromatophores of *Rhodospirillum photometricum*, J. Mol. Biol. 393 (2009) 27–35.
[22] M.L. Cartron, J.D. Olsen, M. Sener, P.J. Jackson, A.A. Brindley, P. Qian, M.J. Dickman, G.J. Leggett, K. Schulten, C. Neil Hunter, Integration of energy and electron transfer processes in the photosynthetic membrane of *Rhodobacter sphaeroides*, Biochim. Biophys. Acta (BBA) — Bioenerg. (2014), http://dx.doi.org/10.1016/j.bbabio.2014.02.003 (in press).
[23] E. Shimoni, O. Rav-Hon, I. Ohad, V. Brumfeld, Z. Reich, Three-dimensional organization of higher-plant chloroplast thylakoid membranes revealed by electron tomography, Plant Cell 17 (2005) 2580–2586.
[24] R. Nevo, D. Charuvi, E. Shimoni, R. Schwarz, A. Kaplan, I. Ohad, Z. Reich, Thylakoid membrane perforations and connectivity enable intracellular traffic in cyanobacteria, EMBO J. 26 (2007) 1467–1473.
[25] R. Nevo, S.G. Chuartzman, O. Tsabari, Z. Reich, D. Charuvi, E. Shimoni, Architecture of thylakoid membrane networks, in: H. Wada, N. Murata (Eds.), Lipids in Photosynthesis, Springer, Netherlands, 2009, pp. 295–328.
[26] D. Charuvi, V. Kiss, R. Nevo, E. Shimoni, Z. Adam, Z. Reich, Gain and loss of photosynthetic membranes during plastid differentiation in the shoot apex of *Arabidopsis*, Plant Cell Online 24 (2012) 1143–1157.
[27] M. Konorty, V. Brumfeld, A. Vermeglio, N. Kahana, O. Medalia, A. Minsky, Photosynthetic system in *Blastochloris viridis* revisited, Biochemistry 48 (2009) 4753–4761.
[28] I. Casuso, S. Scheuring, Automated setpoint adjustment for biological contact mode atomic force microscopy imaging, Nanotechnology 21 (2010) 035104.
[29] S.G. Chuartzman, R. Nevo, E. Shimoni, D. Charuvi, V. Kiss, I. Ohad, V. Brumfeld, Z. Reich, Thylakoid membrane remodeling during state transitions in *Arabidopsis*, Plant Cell 20 (2008) 1029–1039.
[30] D. Kaftan, V. Brumfeld, R. Nevo, A. Scherz, Z. Reich, From chloroplasts to photosystems: *in situ* scanning force microscopy on intact thylakoid membranes, EMBO J. 21 (2002) 6146–6153.
[31] R.P. Gonçalves, A. Bernadac, J.N. Sturgis, S. Scheuring, Architecture of the native photosynthetic apparatus of *Phaeospirillum molischianum*, J. Struct. Biol. 152 (2005) 221–228.
[32] L.N. Liu, T.J. Aartsma, R.N. Frese, Dimers of light-harvesting complex 2 from *Rhodobacter sphaeroides* characterized in reconstituted 2D crystals with atomic force microscopy, FEBS J. 275 (2008) 3157–3166.
[33] S. Scheuring, J. Seguin, S. Marco, D. Lévy, B. Robert, J.L. Rigaud, Nanodissection and high-resolution imaging of the *Rhodopseudomonas viridis* photosynthetic core complex in native membranes by AFM, Proc. Natl. Acad. Sci. U. S. A. 100 (2003) 1690–1693.
[34] S. Scheuring, J.N. Sturgis, Chromatic adaptation of photosynthetic membranes, Science 309 (2005) 484–487.
[35] L.N. Liu, K. Duquesne, F. Oesterhelt, J.N. Sturgis, S. Scheuring, Forces guiding assembly of light-harvesting complex 2 in native membranes, Proc. Natl. Acad. Sci. U. S. A. 108 (2011) 9455–9459.
[36] S. Scheuring, J.N. Sturgis, Dynamics and diffusion in photosynthetic membranes from *Rhodospirillum photometricum*, Biophys. J. 91 (2006) 3707.
[37] S. Scheuring, J.N. Sturgis, V. Prima, A. Bernadac, D. Lévy, J.L. Rigaud, Watching the photosynthetic apparatus in native membranes, Proc. Natl. Acad. Sci. U. S. A. 101 (2004) 11293–11297.
[38] S. Scheuring, J.L. Rigaud, J.N. Sturgis, Variable LH2 stoichiometry and core clustering in native membranes of *Rhodospirillum photometricum*, EMBO J. 23 (2004) 4127–4133.
[39] S. Scheuring, R.P. Gonçalves, V. Prima, J.N. Sturgis, The photosynthetic apparatus of *Rhodopseudomonas palustris*: structures and organization, J. Mol. Biol. 358 (2006) 83–96.

[40] D.E. Chandler, J. Gumbart, J.D. Stack, C. Chipot, K. Schulten, Membrane curvature induced by aggregates of LH2s and monomeric LH1s, Biophys. J. 97 (2009) 2978–2984.
[41] C.N. Hunter, J.D. Pennoyer, J.N. Sturgis, D. Farrelly, R.A. Niederman, Oligomerization states and associations of light-harvesting pigment–protein complexes of *Rhodobacter sphaeroides* as analyzed by lithium dodecyl sulfate-polyacrylamide gel electrophoresis, Biochemistry 27 (1988) 3459–3467.
[42] J.D. Olsen, J.D. Tucker, J.A. Timney, P. Qian, C. Vassilev, C.N. Hunter, The organization of LH2 complexes in membranes from *Rhodobacter sphaeroides*, J. Biol. Chem. 283 (2008) 30772–30779.
[43] C.S. Ting, C. Hsieh, S. Sundararaman, C. Mannella, M. Marko, Cryo-electron tomography reveals the comparative three-dimensional architecture of *Prochlorococcus*, a globally important marine cyanobacterium, J. Bacteriol. 189 (2007) 4485–4493.
[44] T. Geyer, V. Helms, A spatial model of the chromatophore vesicles of *Rhodobacter sphaeroides* and the position of the cytochrome bc1 complex, Biophys. J. 91 (2006) 921–926.
[45] S.C. Holt, A.G. Marr, Location of chlorophyll in *Rhodospirillum rubrum*, J. Bacteriol. 89 (1965) 1402–1412.
[46] K.D. Gibson, Nature of the insoluble pigmented structures (chromatophores) in extracts and lysates of *Rhodopseudomonas spheroides*, Biochemistry 4 (1965) 2027–2041.
[47] P. Joliot, A. Joliot, A. Verméglio, Fast oxidation of the primary electron acceptor under anaerobic conditions requires the organization of the photosynthetic chain of *Rhodobacter sphaeroides* in supercomplexes, Biochim. Biophys. Acta 1706 (2005) 204–214.
[48] S. Scheuring, F. Francia, J. Busselez, B.A. Melandri, J.L. Rigaud, D. Lévy, Structural role of PufX in the dimerization of the photosynthetic core complex of *Rhodobacter sphaeroides*, J. Biol. Chem. 279 (2004) 3620–3626.
[49] P. Qian, C.N. Hunter, P.A. Bullough, The 8.5 Å projection structure of the core RC–LH1–PufX dimer of *Rhodobacter sphaeroides*, J. Mol. Biol. (2005) 948–960.
[50] C. Jungas, J.L. Ranck, J.L. Rigaud, P. Joliot, A. Verméglio, Supramolecular organization of the photosynthetic apparatus of *Rhodobacter sphaeroides*, EMBO J. 18 (1999) 534–542.
[51] P. Qian, P.A. Bullough, C.N. Hunter, Three-dimensional reconstruction of a membrane-bending complex: the RC–LH1–PufX core dimer of *Rhodobacter sphaeroides*, J. Biol. Chem. 283 (2008) 14002–14011.
[52] J. Hsin, J. Gumbart, L.G. Trabuco, E. Villa, P. Qian, C.N. Hunter, K. Schulten, Protein-induced membrane curvature investigated through molecular dynamics flexible fitting, Biophys. J. 97 (2009) 321–329.
[53] L.N. Liu, J.N. Sturgis, S. Scheuring, Native architecture of the photosynthetic membrane from *Rhodobacter veldkampii*, J. Struct. Biol. 173 (2011) 138–145.
[54] D.-W. Lee, Y. Öztürk, A. Osyczka, J.W. Cooley, F. Daldal, Cytochrome bc1–cy fusion complexes reveal the distance constraints for functional electron transfer between photosynthesis components, J. Biol. Chem. 283 (2008) 13973–13982.
[55] K. Woronowicz, D. Sha, R.N. Frese, R.A. Niederman, The accumulation of the light-harvesting 2 complex during remodeling of the *Rhodobacter sphaeroides* intracytoplasmic membrane results in a slowing of the electron transfer turnover rate of photochemical reaction centers, Biochemistry 50 (2011) 4819–4829.
[56] R.K. Clayton, The induced synthesis of catalase in *Rhodopseudomonas spheroides*, Biochim. Biophys. Acta 37 (1960) 503–512.
[57] H. Kirchhoff, C. Hall, M. Wood, M. Herbstová, O. Tsabari, R. Nevo, D. Charuvi, E. Shimoni, Z. Reich, Dynamic control of protein diffusion within the granal thylakoid lumen, Proc. Natl. Acad. Sci. 108 (2011) 20248–20253.
[58] E. Iannuccelli, F. Mompart, J. Gellin, Y. Lahbib-Mansais, M. Yerle, T. Boudier, NEMO: a tool for analyzing gene and chromosome territory distributions from 3D-FISH experiments, Bioinformatics 26 (2010) 696–697.
[59] W.S. Rasband, ImageJ, U.S. National Institutes of Health, Bethesda, Maryland, USA, 1997–2013. (http://rsbweb.nih.gov/ij/).
[60] J.N. Sturgis, R.A. Niedermann, The effect of different levels of the B800–850 light-harvesting complex on intracytoplasmic membrane development in *Rhodobacter sphaeroides*, Arch. Microbiol. 165 (1996) 235–242.
[61] G. Binnig, C.F. Quate, C. Gerber, Atomic force microscope, Phys. Rev. Lett. 56 (1986) 930–933